PNAS RESEARCH ARTICLE | IMMUNOLOGY AND INFLAMMATION

EBF1 is continuously required for stabilizing local chromatin accessibility in pro-B cells

Nikolay Zolotarev[a], Marc Bayer[a], and Rudolf Grosschedl[a,1]

Edited by Ellen Rothenberg, California Institute of Technology, Pasadena, CA; received June 21, 2022; accepted September 29, 2022

The establishment of de novo chromatin accessibility in lymphoid progenitors requires the "pioneering" function of transcription factor (TF) early B cell factor 1 (EBF1), which binds to naïve chromatin and induces accessibility by recruiting the BRG1 chromatin remodeler subunit. However, it remains unclear whether the function of EBF1 is continuously required for stabilizing local chromatin accessibility. To this end, we replaced EBF1 by EBF1-FKBP^{F36V} in pro-B cells, allowing the rapid degradation by adding the degradation TAG13 (dTAG13) dimerizer. EBF1 degradation results in a loss of genome-wide EBF1 occupancy and EBF1-targeted BRG1 binding. Chromatin accessibility was rapidly diminished at EBF1-binding sites with a preference for sites whose occupancy requires the pioneering activity of the C-terminal domain of EBF1. Diminished chromatin accessibility correlated with altered gene expression. Thus, continuous activity of EBF1 is required for the stable maintenance of the transcriptional and epigenetic state of pro-B cells.

EBF1 | BRG1 | dTAG | chromatin accessibility | B cell

"Pioneer" transcription factors (TFs) play an important role in programming cell type-specific gene expression profiles. These TFs can bind closed chromatin and establish an accessible chromatin context for other DNA-binding proteins (reviewed in refs. 1–3). Studies of interactions of pioneer TFs with nucleosomal DNA indicated different modes of binding and different mechanisms of generating local accessibility (1). Pioneer TFs have been found to evict nucleosomes, partially unwrap DNA from nucleosomes, and recruit ATP-dependent chromatin remodeling complexes (4–7). Moreover, cooperative interactions of pioneer TFs with other TFs allow for cell type-specific gene expression (8). Thus, pioneer TFs have been implicated in alterations of gene networks during developmental transitions (reviewed in refs. 1 and 3).

The cell type-specific pioneer TF early B cell factor 1 (EBF1) acts as a key determinant in programming the B lineage. EBF1 acts in a regulatory network with other cell type-specific TFs to activate the B cell program and to antagonize the expression of alternative lineage potential (reviewed in refs. 9–11). A time course study of chromatin binding by EBF1 and the formation of local accessibility has shown that EBF1 binds naïve progenitor chromatin well before the appearance of detectable chromatin accessibility and the onset of gene expression (12). This and other studies also provided evidence for hierarchical networks of TFs in which PU.1 and Ikaros function in multipotent progenitors, whereas EBF1 and E2A act upstream of PAX5 in specifying the B cell lineage (13–15). The activation of B lineage-specific gene expression also requires the function of BRG1, a catalytic subunit of the SWI/SNF chromatin-remodeling complex (reviewed in ref. 16), which is recruited to EBF1-bound sites by interaction with the C-terminal domain of EBF1 (17, 18). This protein domain of EBF1 also enables liquid-liquid phase separation and is important for the "pioneering" activity of EBF1 (18, 19). BRG1 recruitment stabilizes chromatin binding by EBF1, whereby the CTD is specifically required for EBF1 binding at a set of "CTD-dependent sites" that differ from "CTD-independent sites" by the lack of neighboring TF-binding sites that enable cooperative chromatin binding (18, 19).

The recent analysis aimed at elucidating the dynamics of SWI/SNF function by inducible protein degradation or pharmacological inhibition showed that the loss of SWI/SNF activity results in a rapid closure of active chromatin (20, 21). To address the question of whether or not the maintenance of stable chromatin accessibility also requires a continuous function of pioneer TFs, we adopted the degradation TAG (dTAG) system for inducible degradation of EBF1, tagged with FK506-binding protein (FKBP) (22–24). Here, we report that EBF1 is required for continuous BRG1 recruitment and maintenance of open chromatin regions. Notably, we found that the elimination of EBF1 results in preferential chromatin closure at CTD-dependent sites, suggesting that the cooperation of EBF with other TFs may alleviate the need for continuous pioneering function.

Significance

EBF1 is a key determinant of a transcriptional regulatory network involved in establishing the B cell fate by activating lineage-specific gene expression and repressing genes associated with alternative cell fates. In this regulatory network, EBF1 acts as a pioneer TF that is able to bind naïve progenitor chromatin and establish local chromatin accessibility by recruiting BRG1. Here, we show that the dTAG-induced degradation of EBF1 in pro-B cells results in a rapid loss of BRG1 recruitment and chromatin accessibility at EBF1-binding sites, accompanied by altered target gene expression. Thus, the continuous activity of EBF1 is required to stabilize and maintain the B lineage gene expression program.

Author affiliations: [a]Max Planck Institute of Immunobiology and Epigenetics, Freiburg 79108, Germany

Author contributions: N.Z., M.B., and R.G. designed research; N.Z. and M.B. performed research; N.Z. and R.G. analyzed data; and N.Z. and R.G. wrote the paper.

The authors declare no competing interest.

This article is a PNAS Direct Submission.

[1]To whom correspondence may be addressed. Email: grosschedl@ie-freiburg.mpg.de.

This article contains supporting information online at https://www.pnas.org/lookup/suppl/doi:10.1073/pnas.2210595119/-/DCSupplemental.

Published November 21, 2022.

Results

dTAG-induced Degradation of EBF1. To allow for a rapid dTAG-induced EBF1 protein degradation, we fused the $FKBP12^{F36V}$ degradation tag onto the amino (N) or carboxyl (C) terminus of EBF1 and inserted these gene constructs into bicistronic retroviral vectors that express the tagged EBF1 proteins along with GFP (Fig. 1*A*). To generate pro-B cells in which the endogenous EBF1 protein has been replaced by the $FKBP12^{F36V}$-tagged EBF1 proteins, termed EBF1-FKBP(N) and EBF1-FKBP(C), we transduced A-MuLV-transformed *Ebf1*$^{fl/fl}$*RERT*^{Cre} pro-B cells with the bicistronic retroviruses and subsequently deleted the endogenous *Ebf1* alleles by treating cells with tamoxifen (*SI Appendix*, Fig. S1*A*) (19). This experimental strategy allows for the expression of modified EBF1 proteins at levels similar to that of endogenous EBF1 protein. Immunoblot analysis of lysates of EBF1-FKBP-expressing cells with the monoclonal α-EBF1 (6G6) antibody indicated that the tagged proteins migrated slower than endogenous EBF1, whereby we detected similar expression levels of the EBF1wt and EBF1-FKBP proteins (Fig. 1 *B*, *Top panel*). We induced EBF1 degradation in EBF1-FKBP-expressing cells by adding the bifunctional molecule dTAG13, which links the $FKBP^{F36V}$ tag with the cereblon ubiquitin E3 ligase (23). At 2 h, 4 h, and 24 h after dTAG13 addition, we assessed protein levels by immunoblot analysis and found that both N- and C-terminal tagged EBF1 protein levels were markedly reduced already after 2 h (Fig. 1*C*).

To examine the effects of dTAG13 addition on the occupancy of EBF1 at genomic loci, we performed quantitative chromatin immunoprecipitation (ChIP) and determined EBF1 binding at 0 h, 6 h, and 24 h. For the ChIP assay of EBF1-FKBP(C), we used the ChIP-grade polyclonal α-EBF1 (1C) antibodies, which recognize an N-terminal EBF1 peptide (25, 26). These antibodies bind efficiently EBF1-FKBP(C) but not EBF1-FKBP(N), most likely due to an interference with the N-terminal FKBP tag (Fig. 1 *B*, *Middle panel*). For the analysis of EBF1 occupancy upon dTAG13-induced degradation, we chose genomic sites that are bound by EBF1 in a CTD-dependent or CTD-independent manner. We have previously shown that the CTD is required for EBF1 binding to sites in the context of a few neighboring TF-binding motifs, whereas the CTD is dispensable at sites with many flanking TF-binding motifs (19). Notably, we observed a similar loss of EBF1 binding at CTD-independent and CTD-dependent sites at 6 h (Fig. 1*D*). At a few sites, we detected an additional modest reduction of EBF1 occupancy after 24 h of dTAG13 addition.

To confirm these data with the N-terminal-tagged EBF1-FKBP(N), we used the α-FLAG antibody, which yielded lower signal-to-noise ratios but confirmed the decrease of EBF1 occupancy at CTD-dependent and CTD-independent sites (*SI Appendix*, Fig. S1 *B* and *C*). Thus, the elimination of chromatin-bound EBF1 after induced degradation occurs regardless of the position of the FKBP tag. We also assessed the genome-wide effects of targeted EBF1-FKBP(C) degradation on EBF1 occupancy by performing ChIP-seq analysis with the α-EBF1 (1C) antibodies. To interrogate the effects of EBF1 degradation on binding at CTD-dependent and CTD-independent sites, we plotted the profiles of the EBF1 peaks onto previously identified sets of sites occupied by EBF1ΔCTD and/or EBF1wt (18). This analysis revealed a markedly reduced EBF1 occupancy at the vast majority of all EBF1-binding sites, irrespective of their dependence on the CTD (Fig. 1 *E* and *F*). The efficient elimination of EBF1 from chromatin sites was confirmed for individual CTD-independent genes (*Igll1* and *Cd19*) and CTD-dependent genes (*Asb2* and *Cd72*) (Fig. 1*G* and *SI Appendix*, Fig. S1*D*). Taken together, these data revealed an efficient elimination of chromatin-bound EBF1 at both CTD-dependent and CTD-independent sites.

Depletion of EBF1 Leads to a Loss of BRG1 Binding and Rapid Chromatin Closure. We have previously shown that EBF1 is able to recruit BRG1, thereby facilitating local chromatin opening in naïve progenitor chromatin (18). The interaction with BRG1 requires the CTD of EBF1, which contains a PLD enabling liquid-liquid phase separation (18). To examine the effects of induced EBF1 degradation on BRG1 binding at EBF1-binding sites, we performed quantitative ChIP assays with EBF1-FKBP(N)-expressing pro-B cells to avoid a potential interference of a C-terminal FKBP tag with the CTD function. We detected reduced BRG1 binding at both CTD-dependent and CTD-independent sites already at 6 h with no further change at 24 h (Fig. 2*A*). Consistent with the impaired BRG1 association at EBF1-binding sites in dTAG13-treated cells, we also observed a reduction in DNase I hypersensitivity after 6 h (Fig. 2*B*).

To extend the analysis of BRG1 recruitment and local chromatin accessibility to the entire genome, we performed BRG1 ChIP-seq and ATAC-seq with untreated and dTAG13-treated EBF1-FKBP(N)-expressing cells. The analysis of BRG1 binding at sites of CTD-dependent and CTD-independent EBF1 occupancy indicated a reduction of BRG1 peaks at 6 h of dTAG13 treatment relative to the untreated condition, whereby the reduction of BRG1 binding was more pronounced at CTD-dependent sites than at CTD-independent sites (Fig. 2 *C* and *D*). No change of BRG1 binding was detected at sites lacking EBF1 occupancy.

By ATAC-seq analysis of untreated cells, we identified 50,003 accessible regions that did not coincide with sites of EBF1 occupancy and 5,202 accessible regions that overlapped with EBF1-bound sites. In dTAG13-treated cells, we detected a marked loss of accessibility at CTD-dependent sites and a decrease in accessibility at CTD-independent sites (Fig. 2 *E* and *F*). The vast majority of accessible regions lacking EBF1 occupancy did not change upon dTAG13 treatment (Fig. 2 *E* and *F*). The different effects of EBF1 degradation on the recruitment of BRG1 and local chromatin accessibility at CTD-dependent and CTD-independent sites of EBF1 occupancy were also observed at individual genes (*Car2*, *Cd19*) (Fig. 2 *G* and *H*).

To confirm these data, we also examined the effects of dTAG13 treatment on BRG1 recruitment and local chromatin accessibility in EBF1-FKBP(C)-expressing cells. We observed a similar decrease in gene-specific BRG1 recruitment and DNAse I hypersensitivity as in EBF1-FKBP(N)-expressing cells (*SI Appendix*, Fig. S2 *A* and *B*). The elimination of BRG1 from EBF1-binding sites was even more noticeable in EBF1-FKBP(N)-expressing cells suggesting a possible interference of the FKBP tag with the CTD in its association with BRG1. Moreover, the genome-wide analysis of ATAC peaks in dTAG13-treated EBF1-FKBP(C)-expressing cells confirmed the preferential local chromatin closure at CTD-dependent sites (*SI Appendix*, Fig. S2 *C* and *D*). The ATAC peak intensities at CTD-dependent EBF1 target sites were lower than those in EBF1-FKBP(N)-expressing cells, although the overall sizes and changes of ATAC peaks were similar in both data sets (*SI Appendix*, Fig. S2 *E* and *F*). In dTAG13-treated EBF1-FKBP(N)-expressing cells, we generally detected more altered peaks than in corresponding EBF1-FKBP(C)-expressing cells (*SI Appendix*, Fig. S2*G*). Many of the gained ATAC-peaks in dTAG13-treated EBF1-FKBP(N) cells did not overlap with EBF1-binding sites in dTAG13-treated EBF1-FKBP(N) cells (*SI Appendix*, Fig. S2*G*), which could reflect indirect chromatin changes as a consequence of altered gene expression. Taken together, these data indicate that

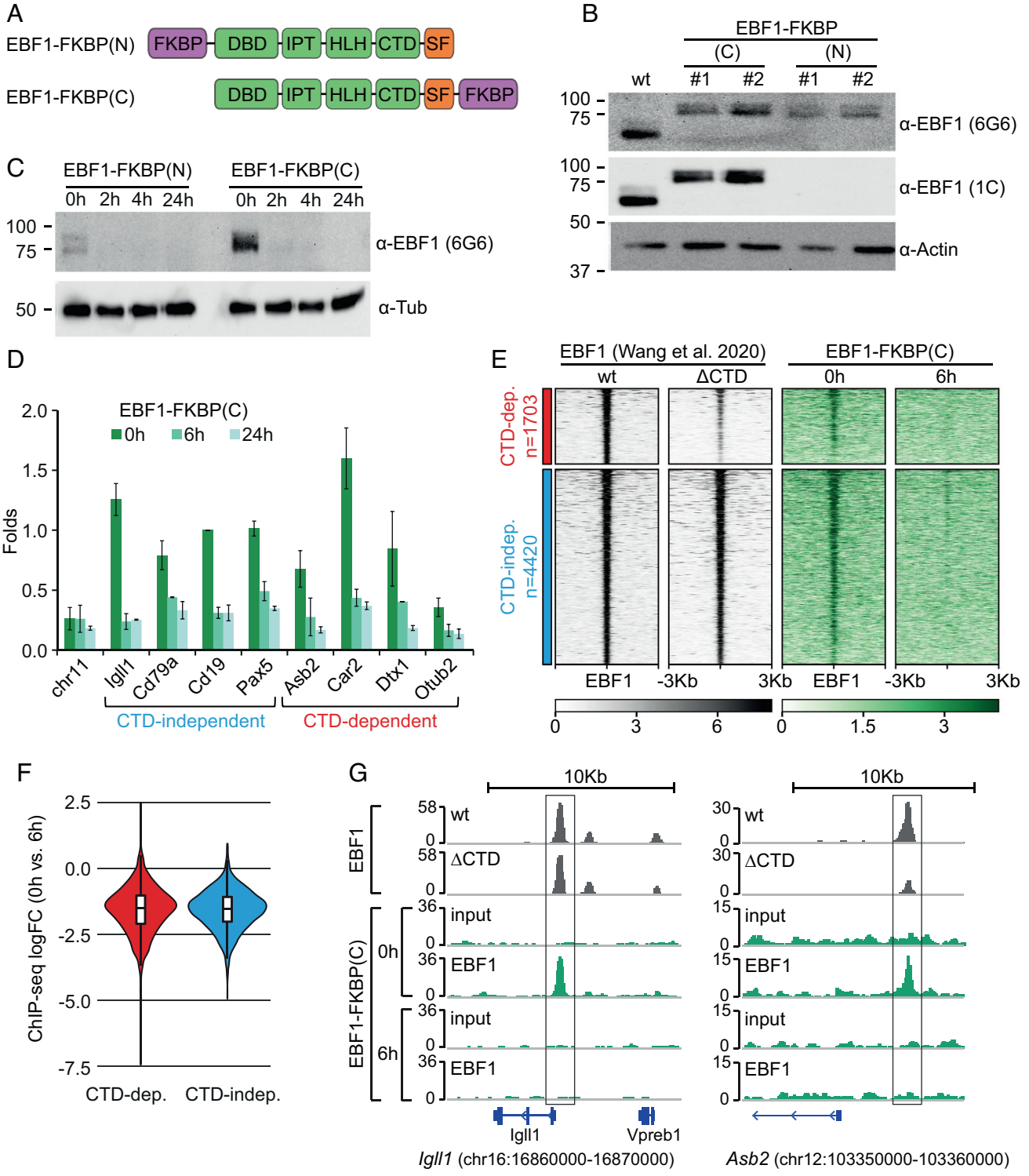

Fig. 1. dTAG13 allows for efficient depletion of EBF1 in cells and on chromatin. (*A*) Schematic representation of EBF1-FKBP constructs with protein domains indicated. (FKBP, F36V; DBD, DNA-binding domain; IPT, Ig-like plexin TF; HLH, helix-loop-helix; CTD, C-terminal domain; SF, Strep-FLAG. (*B*) Immunoblot analysis to detect EBF1 expression in A-MuLV pro-B cells and in two independent clones expressing EBF1-FKBP(C) or EBF1-FKBP(N). For the detection of EBF1 and the EBF1 fusion proteins, the monoclonal α-EBF1 (6G6) antibody and the polyclonal α-EBF1 (1C) antibodies were used. Actin is a loading control. (*C*) Immunoblot analysis to detect expression of EBF1-FKBP(N) and EBF1-FKBP(C) in pro-B cells after treatment with dTAG13 for 2, 4, and 24 h. Tubulin is a loading control. (*D*) ChIP-qPCR analysis of chromatin binding of EBF1-FKBP(C) at CTD-dependent and CTD-independent sites after treatment of cells with dTAG13 for 6 or 24 h. Bars represent means and error bars represent SD of two biological replicates. (*E*) Heatmap of ChIP-seq with α-EBF1 antibody (1C). *Left-hand Panels*: Chromatin binding of EBF1wt and EBF1ΔCTD in pro-B cells (18). CTD-dependent sites are defined by more than twofold lower binding efficiency of EBF1ΔCTD relative to EBF1wt. *Right-hand Panels*: Binding of EBF1-FKBP(C) at CTD-dependent and CTD-independent sites before and after treatment with dTAG13 for 6 h. Profiles of the EBF1 peaks were plotted onto previously identified CTD-dependent and CTD-independent sites (18). (*F*) Violin plot of the log-fold change of EBF1 occupancy at CTD-dependent (red) and CTD-independent (blue) sites as determined in Fig. 1*E*. (*G*) Genome browser tracks showing EBF1 occupancy at representative genes for CTD-independent (*Igll1*) and CTD-dependent (*Asb2*) target sites. Data on EBF1wt and EBF1ΔCTD occupancy are from Wang et al., 2020 (18).

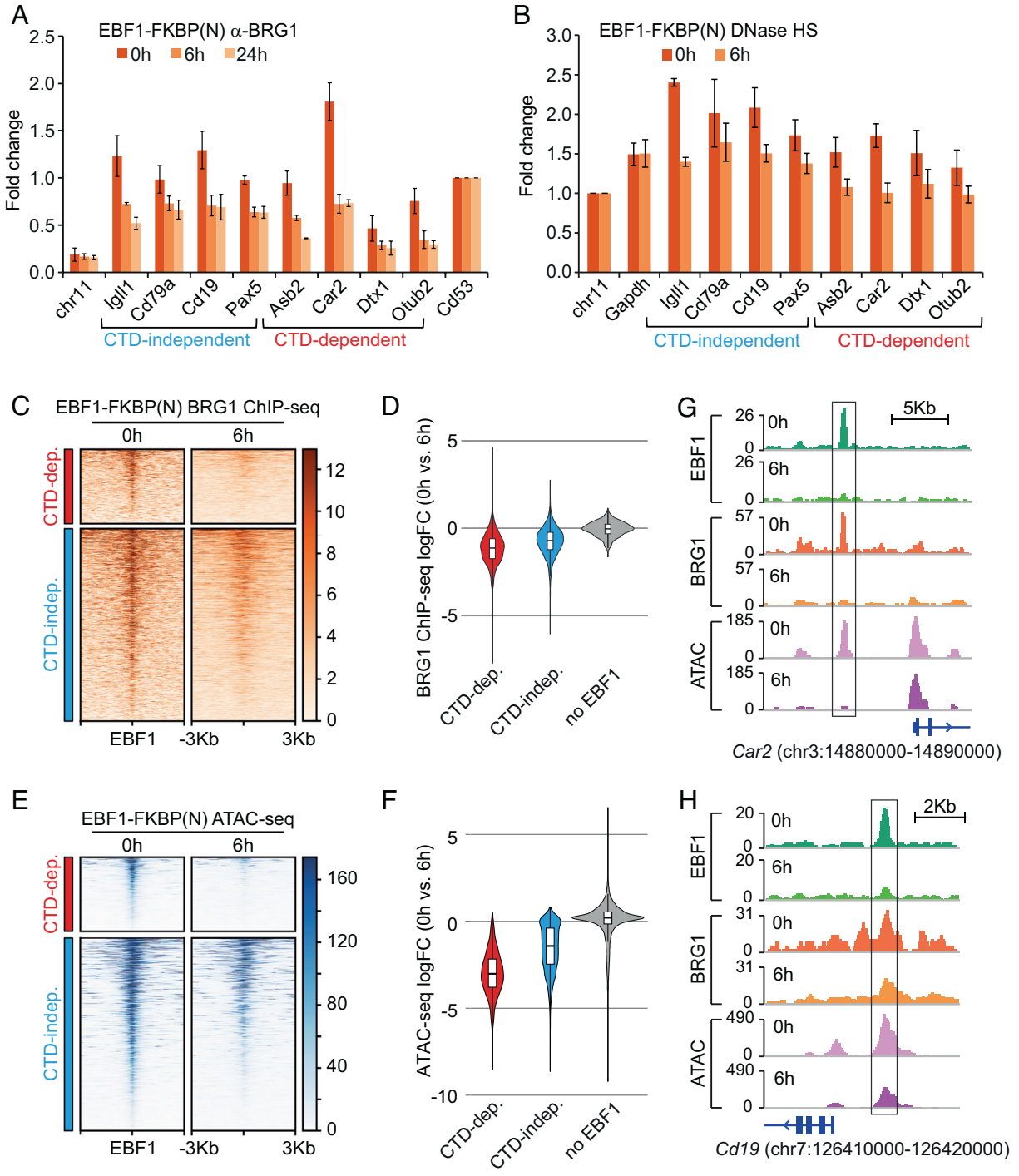

Fig. 2. Depletion of EBF1 leads to a decrease in BRG1 recruitment to EBF1 sites and local chromatin closure. (*A*) ChIP-qPCR to detect BRG1 binding at CTD-dependent and CTD-independent example genes in untreated or dTAG13-treated EBF1-FKBP(N)-expressing pro-B cells. Bars represent means and error bars represent SD of two biological replicates. Cells were treated for 6 or 24 h. (*B*) Analysis of DNase I hypersensitive sites at representative genes in EBF1-FKBP(N) pro-B cells after treatment with dTAG13 for 6 h. Bars represent means and error bars represent SD of two biological replicates. (*C*) Heatmap of ChIP-seq with α-BRG1 antibody in EBF1-FKBP(N) cells before and after treatment with dTAG13 for 6 h. BRG1 binding profiles were plotted on CTD-dependent and CTD-independent EBF1 sites, as described in Fig. 1*E*. (*D*) Violin plot of the log-fold change of BRG1 occupancy (from Fig. 2*C*) at CTD-dependent (red), CTD-independent (blue) EBF1-binding sites, and EBF1-independent sites (gray). (*E*) Heatmap of ATAC-seq analysis in EBF1-FKBP(N) cells before and after treatment with dTAG13 for 6 h. ATAC-seq profiles were plotted on CTD-dependent and CTD-independent EBF1 sites, as described in Fig. 1*E*. (*F*) Violin plot of the log-fold changes of ATAC-seq signal (from Fig. 2*E*). (*G* and *H*) Genome browser tracks showing EBF1 and BRG1 occupancy and ATAC profiles at representative genes for CTD-dependent (*Car2*) and CTD-independent (*Cd19*) target sites.

the accessibilities of CTD-dependent and CTD-independent sites are differentially affected despite the similar elimination of EBF1 occupancy in dTAG13-treated cells.

The relatively modest change of accessibility of CTD-independent sites may be related to compensatory functions of TFs bound in the vicinity of CTD-independent EBF1-binding sites (19). Therefore, we interrogated publicly available TF binding data in pro-B cells and detected a preferential binding of PU.1, Ikaros and FOXO1 at CTD-independent sites, whereas binding of E2A and PAX5 was similar at CTD-dependent and CTD-independent sites (Fig. 3*A*). As an example for the differential sensitivity of ATAC peaks to the loss of EBF1, one EBF1-associated ATAC peak in the *Ccr7* gene

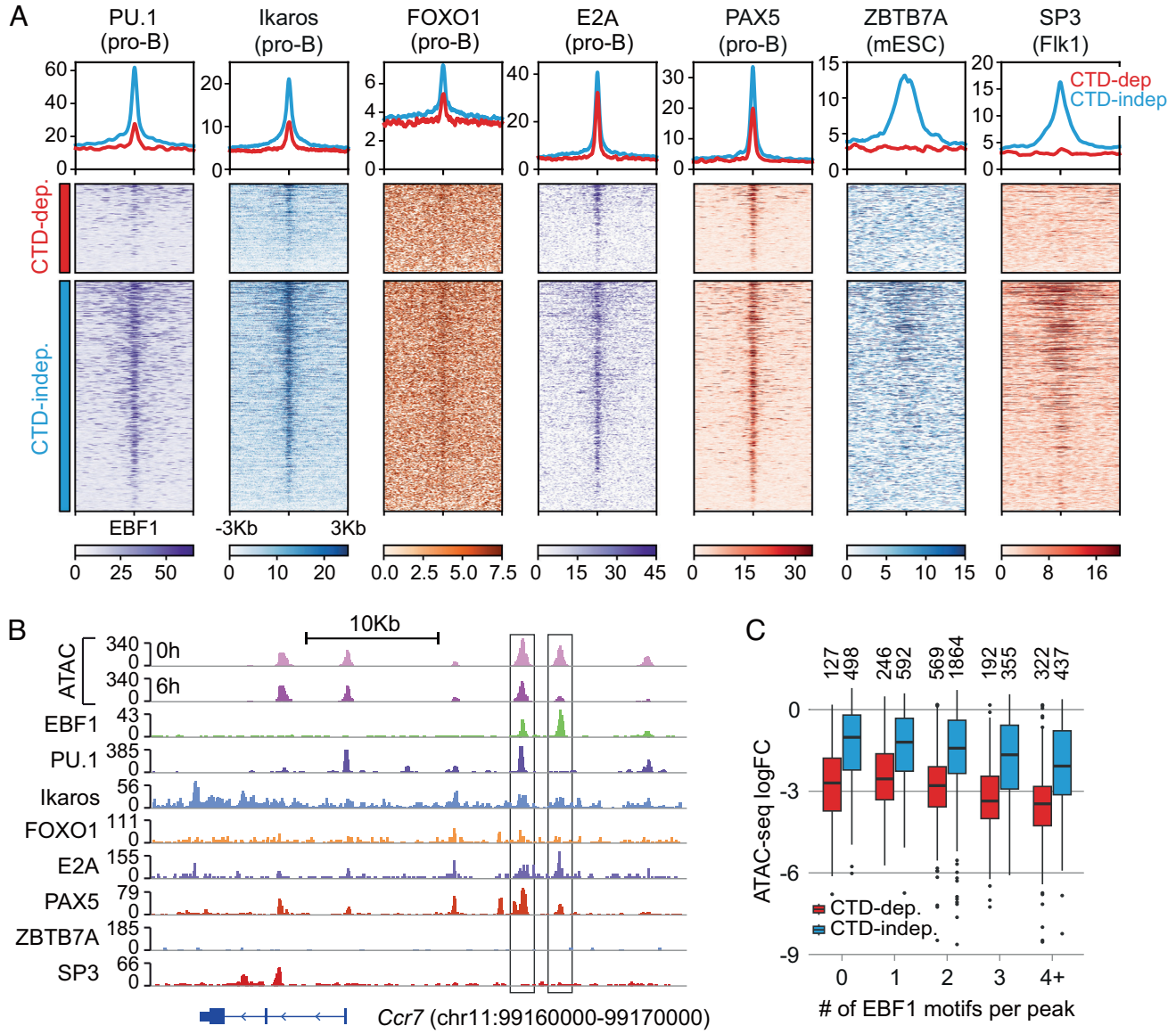

Fig. 3. Co-occupancy of EBF1 with other TFs at CTD-independent sites. (*A*) Heatmap of publicly available ChIP-seq data of TFs to assess their occupancy of CTD-dependent and CTD-independent sites: PU.1 (27); Ikaros (28); FOXO1 and E2A (15); PAX5 (29). ZBTB7A in mESC (30). SP3 in Flk1 cells (31). CTD-dependent and CTD-independent sites are the same as in Fig. 1*E* (18). (*B*) Genome browser tracks showing TF occupancy (as in Fig. 3*A*) and ATAC peaks at the *Ccr7* gene in EBF1-FKBP(N) cells before and after treatment with dTAG13 for 6 h. (*C*) Box plots showing log-fold changes of ATAC-seq peaks in EBF1-FKBP(N) cells in relation with different numbers of EBF1-binding motifs in CTD-dependent (red) or CTD-independent (blue) genes. The numbers of ATAC peaks in each group are depicted on *Top*. The box represents the first and third quartiles with the horizontal line showing the median.

locus that was also bound by PU.1 and PAX5 was retained, whereas a neighboring ATAC peak without PU.1 and PAX5 occupancy was markedly diminished (Fig. 3*B*). Further bioinformatic analysis of ATAC peaks at sites of EBF1 occupancy revealed the predominant presence of one or two EBF1-binding motifs, although a group of CTD-independent sites was found to lack EBF1 motifs (Fig. 3*C*). Notably, the preferential reduction of ATAC peaks at CTD-dependent sites versus CTD-independent sites was independent of the number of EBF1 motifs, although the extent of ATAC peak reduction correlated with the number of EBF1 motifs (Fig. 3*C*). Thus, the presence and occupancy of neighboring TFs at CTD-independent sites may diminish chromatin closure upon EBF1 degradation.

Rapid Changes in Target Gene Expression after EBF1 Depletion. The rapid dTAG-induced degradation of TFs has been used to identify direct target genes (32). For the identification of direct target genes of EBF1, we used strand-specific ribo-zero total RNA-seq to obtain both mature and nascent transcripts instead of all polyadenylated transcripts (33). By counting reads only in exonic regions or over the entire genes, we were able to distinguish between mature and nascent transcripts. After 6 h of dTAG13 treatment of EBF1-FKBP(N)-expressing pro-B cells, 308 genes were more than twofold up- or downregulated relative to untreated cells (*SI Appendix*, Fig. S3*A*). By using intronic reads, we detected a similar number of deregulated genes that largely overlapped with those detected by exonic reads (*SI Appendix*, Fig. S3*B*). To better define differences between exonic and intronic reads, we assessed all significantly deregulated genes without setting a fold threshold (Fig. 4*A*). For a large group of 1,470 genes, both intronic and exonic counts changed in the same ways (in a diagonal axis). For this group of genes, a 6 h treatment with dTAG13 resulted in significant changes of both nascent and mature RNA. For a set of 397 genes, we

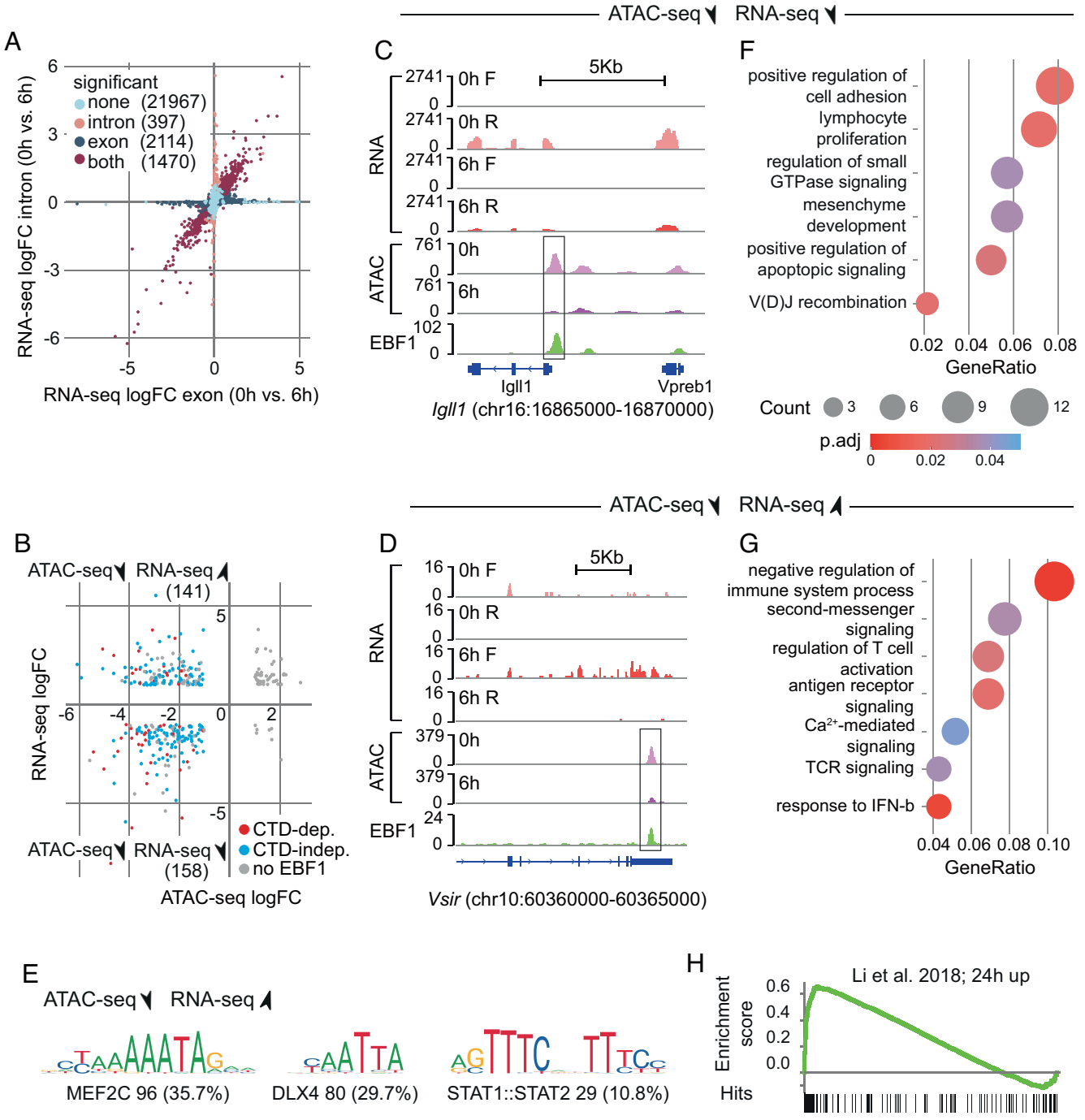

Fig. 4. Depletion of EBF1 leads to rapid deregulation of EBF1 target gene expression. (*A*) Correlation between exonic and intronic log-fold changes for RNA-seq in EBF1-FKBP(N) cells before and after treatment with dTAG13 for 6 h. Data were subsampled for visualization. (*B*) Integration of RNA-seq and ATAC-seq analysis by assessing differentially expressed genes (logFC > 1, padj < 0.05) with differential ATAC peaks (logFC >1, FDR < 0.05) within 100 kbp from TSS. For each gene, one differential ATAC peak with the lowest FDR was selected. Genes with CTD-dependent (red), CTD-independent (blue), or no (gray) EBF1 sites are shown. The lower-left quadrant includes genes with diminished ATAC peaks and downregulated expression (genes activated by EBF1). The Upper-left quadrant includes genes with diminished ATAC peaks and upregulated expression in dTAG13-treated cells (genes repressed by EBF1). (*C* and *D*) Genome browser tracks of RNA expression and ATAC profiles of example genes (*Igll1*, *Vsir*) in EBF1-FKBP(N) cells before and after treatment with dTAG13 for 6 h. (*E*) Selected motifs enriched at the promoters of upregulated genes with decreased ATAC peak. (*F* and *G*) Selected enriched gene ontology (GO) biological process terms. (*H*) Gene set enrichment analysis (GSEA) of genes upregulated after 24 h of EBF1 expression (12).

detected only changes of intron reads, suggesting that only nascent transcripts are affected or that the transcripts contain very large introns. A group of 2,114 genes with differential exon reads was enriched in genes with short introns, such as *Vpreb1,* which has one intron of less than 100 bp. Such short intron sizes may explain the failure to detect changes in intronic counts. Finally, we interrogated the RNA-seq data with ATAC-seq and EBF1 ChIP-seq data to identify direct EBF1 targets and better understand the differential regulation of these genes upon EBF1 degradation. For this analysis, we selected all differential ATAC peaks within 100 kb of the transcription start sites (TSS), because EBF1 is frequently bound at promoter-distal enhancers (26). Among all deregulated genes, 299 genes contained ATAC peaks that were decreased upon EBF1 elimination (Fig. 4*B*). In this gene set, 158 genes were downregulated (activated by EBF1) and 141 genes were upregulated (repressed by EBF1)

(Fig. 4*B* and Dataset S1). Moreover, 80 to 90% of these genes were bound by EBF1 in untreated pro-B cells, identifying the genes as direct EBF1 targets (Dataset S1). A small set of 45 upregulated genes was associated with ATAC peaks that appeared upon EBF1 depletion (Fig. 4*B*). These genes were most likely indirectly deregulated upon EBF1 degradation, because their associated ATAC peaks did not overlap with EBF1 occupancy in untreated pro-B cells (Dataset S1). These patterns of altered gene expression and local chromatin accessibility were also observed for individual genes, including *Igll1* and *Lef1* as representative genes with reduced transcript levels and ATAC peaks (Fig. 4*C* and *SI Appendix*, Fig. S3*C*), *Vsir* and *Ccr7* as representative genes with enhanced expression and reduced ATAC peaks (Fig. 4*D* and *SI Appendix*, Fig. S3*D*), and *Pglyrp2* as a representative upregulated gene with enhanced ATAC peaks (*SI Appendix*, Fig. S3*E*). The observation of impaired chromatin accessibility at EBF1-occupied sites and an increased RNA expression of associated genes upon EBF1 degradation (for example at the *Vsir* and *Ccr7* genes) was at first glance surprising. However, we noted that the reduced chromatin accessibility occurs at promoter-distal sites, whereas the ATAC peaks in the vicinity of the TSS generally increased, consistent with the enhanced RNA expression (*SI Appendix*, Fig. S3*F*). Therefore, the decrease in promoter-distal ATAC peaks upon EBF1 depletion may reflect a reduced activity of EBF1-dependent silencer regions.

To explore the difference between EBF1-mediated activation versus repression of target gene by EBF1, we compared TF-binding motifs at the promoters of genes that were down- or upregulated upon EBF1 depletion. Promoter regions of upregulated genes with decreased ATAC peaks showed a significant enrichment of binding motifs for MEF2C, DLX, and STAT1:STAT2, whereas no considerable enrichment of specific TF-binding motifs was observed in promoter regions of downregulated genes (Fig. 4*E* and *SI Appendix*, Fig. S4*G*).

GO analysis of genes that were downregulated and had reduced ATAC peaks upon EBF1 elimination revealed an enrichment of genes associated with cell adhesion, lymphocyte proliferation and small GTPase signaling (Fig. 4*F* and *SI Appendix*, Table S1). However, many typical B lineage genes, including *Foxo1*, *Pax5*, and *Cd79a,* were more modestly downregulated upon EBF1 depletion (Dataset S1). Interestingly, upregulated genes with reduced ATAC peaks were enriched for gene signatures of T cell and NK cell differentiation and function (Fig. 4*G* and *SI Appendix*, Table S1), which is consistent with the role of EBF1 in the repression of alternative lineage fates in early stages of B cell differentiation (34). Among the small set of upregulated genes with enhanced ATAC peaks that do not overlap with EBF1 occupancy, we observed an enrichment for genes implicated in B cell activation and interferon gamma production (*SI Appendix*, Fig. S4*H* and Table S1).

To compare the data of the deregulation of EBF1-occupied genes after dTAG13 treatment with previously published sets of EBF1 target genes, we used the GSEA. First, we used the data set of genes that are up- or downregulated within 24 h of EBF1 induction in *Ebf1*$^{-/-}$ progenitor cells (12). We found a strong correlation between genes that are downregulated at 6 h of EBF1 degradation and upregulated at 24 h of EBF1 induction (Fig. 4 *H* and Dataset S1). We also observed significant overlap of deregulated genes in dTAG13-treated pro-B cells with a data set of deregulated genes in the pro-B cell stage of EBF1 induction (12) (*SI Appendix*, Fig. S4 *A* and *B*) and with data sets of previous EBF1 gain-of-function and loss-of-function experiments (26) (*SI Appendix*, Fig. S4 *C*–*G*). As expected, genes previously identified as EBF1-activated genes showed a reduced expression upon EBF1 degradation, whereas EBF1-repressed genes were upregulated in dTAG13-treated cells. Taken together, local chromatin closures after dTAG13-induced EBF1 degradation led to the rapid down- and upregulation of EBF1 target genes.

Discussion

In this study, we explored the role of TF EBF1 in conferring stable local chromatin accessibility. We have previously shown that EBF1 functions as a "pioneer" TF that binds to naïve progenitor chromatin prior to the formation of chromatin accessibility (12, 19). The ability of binding to sites of chromatin that are not accessible for cleavages by nucleases or transposases are hallmarks of pioneer TFs (reviewed in ref. 35). The initial binding of pioneer TFs is unstable but it can be stabilized by the recruitment of chromatin remodeling complexes (36, 37) (reviewed in ref. 38). Recently, EBF1 has been found to recruit the BRG1 subunit of the SWI/SNF complex via a C-terminal domain that allows EBF1 to access EBF1-binding sites with few or no neighboring TF-binding sites (18, 19). By using the dTAG13-based protein degradation system, we examined the immediate effects of EBF1 elimination. The analysis of the genome-wide effects of EBF1 degradation on EBF1 occupancy of enhancers, BRG1 binding, chromatin accessibility, and gene expression allowed us to make several conclusions.

First, EBF1 degradation results in a rapid loss of EBF1 occupancy. Notably, we observed a similar loss at CTD-dependent and CTD-independent enhancer and promoter sites, suggesting that EBF1 binding is not stabilized by interactions with other TFs. Although EBF1 has been found to cooperate functionally with other TFs, including E2A (TCF3), RUNX1, PAX5, and MEF2C (39–42), no direct physical interactions between EBF1 and these TFs have been reported. Future experiments will be required to determine the residence time of chromatin-bound EBF1 and establish whether EBF1 degradation affects stable chromatin-bound EBF1 bound or dynamic re-binding of EBF1.

Second, the loss of EBF1 resulted in the diminished binding of BRG1 at both CTD-dependent and CTD-independent sites. In contrast, we observed a differential loss of chromatin accessibility at both sets of EBF1-binding sites. The partial resistance of CTD-independent sites to chromatin closure upon EBF1 elimination may be linked to a compensatory function of other TFs occupying regions of EBF1-binding sites. In particular, the pioneer TFs PU.1, Ikaros, and FOXO1 were found to occupy preferentially CTD-independent regulatory regions. These regions also showed an enrichment of binding motifs for SP3 and LRF (ZBTB7a), a regulator of the B versus T lineage decision (43, 44). In contrast, CTD-dependent regions show a co-occupancy of E2A and PAX5. These TFs act in a regulatory network with EBF1 but they may not be able to compensate for the loss of EBF1 in recruiting BRG1 and maintaining open chromatin.

The requirement of the SWI/SNF chromatin remodeling complex for the stable maintenance of chromatin accessibility has been recently shown by using dTAG-induced degradation of BAF subunits or small molecule inhibitors of SWI/SNF activity in mES cells (20, 21). However, studies of the effects of pioneer TF elimination on local chromatin accessibility have been limited. Auxin-induced degradation of OCT4 at different phases of the cell cycle in ES cells revealed a continuous requirement of OCT4 activity to maintain enhancer accessibility (45). Likewise, continuous activity of the pioneer TF Zelda was found to be required for proper zygotic gene activation in Drosophila (46).

Third, the analysis of the effects of EBF1 degradation on gene expression allowed for the identification of relatively small sets of

genes that were down- or that upregulated and had lost accessibility in regions of EBF1 occupancy in untreated pro-B cells. One hundred and forty-four out of 158 downregulated genes showed EBF1 occupancy in untreated cells, identifying them as direct target genes. Interestingly, this set of genes includes *VpreB1, VpreB2*, *Igll1*, *Fetub*, and *Fam53b*, which were previously identified as genes that are activated immediately after induction of EBF1 expression in *Ebf1*$^{-/-}$ progenitors, prior to the activation of *Pax5* (12). Moreover, this set of downregulated genes encompasses *Bst1* and *Gfra2*, which are activated at the earliest stage of B cell ontogeny (47). These genes represent targets that are regulated by EBF1 prior to the onset of PAX5 expression (12, 47). At a less stringent cutoff of logFC in downregulation, we identified *Pax5*, *Foxo1*, and many typical B cell marker genes, suggesting that these modestly deregulated genes involve a co-regulation by EBF1 and PAX5 and/or other B cell TFs and are therefore less affected by the EBF1 elimination. Conversely, the set of 141 upregulated genes includes EBF1-repressed targets. These genes encode important regulatory and functional determinants of NK and T cells, such as *Itk*, *Lat*, *Ccr7*, *IL12rb1*, *Ltb*, and *Vsir*. Many of the genes have also been previously identified as EBF1-repressed genes, consistent with the function of EBF1 as a safeguard of B lineage identity (26, 34). For most of these genes, we observed a diminished local chromatin accessibility, raising the question of how the impaired chromatin accessibility is associated with augmented gene expression. Notably, the sites of reduced local accessibility did not coincide with promoter-proximal regions but were found in promoter-distal regions. Consistent with the upregulation of gene expression, the ATAC peaks at the TSS of these genes were by and large enhanced. Possibly, a diminished silencing activity of promoter-distal EBF1-dependent regulatory regions may result in the upregulation of gene expression. We did not detect obvious sequence signatures around EBF1-binding sites that might be involved in repressing versus activating functions of EBF1. In the promoter regions of the upregulated gene set, however, we detected an enrichment of binding sites for MEF2C, which has been shown to interact with EBF1 and has been implicated in the repression of myeloid genes in B cells (42). The rapid elimination of EBF1 also uncovered unexpected differences in the dependence of target genes on EBF1 function. Notably, genes that were robustly downregulated upon EBF1 depletion overlapped with genes that are early activated after EBF1 induction in *Ebf1*$^{-/-}$ progenitors, prior to the expression of PAX5. Therefore, these genes may primarily depend on EBF1 function. In contrast, the modest deregulation of genes after EBF1 degradation may reflect a co-regulation of EBF1 with other B lineage TFs.

In conclusion, our analysis showed that EBF1 activity is continuously required for stabilizing local chromatin accessibility and assuring the maintenance of a cell type-specific program of gene expression.

Materials and Methods

dTAG13 Treatment. Cells were resuspended in RPMI medium. dTAG13 was added to the final concentration of 0.5 μM (from 0.5 mM stock in DMSO). The same volume of DMSO was added to the control sample (0 h). For most experiments, cells were incubated with dTAG13 for 6 or 24 h.

ChIP. EBF1 ChIP and BRG1 ChIP were performed according to previous protocols (17, 19), with some changes outlined in *SI Appendix*. Primers used for qPCR are indicated in *SI Appendix*, Table S2).

ATAC-seq and RNA-seq. ATAC-seq was performed using Tagmentation Mix (Diagenode) according to the manufacturer's protocol with some modifications detailed in *SI Appendix*. For RNA-seq, RNA was purified using Qiagen RNeasy Kit according to the manufacturer's protocol. Libraries were prepared using Illumina Stranded Total RNA Prep with Ribo-Zero Plus kit according to the manufacturer's protocol.

Quantification and Statistical Analysis. Peak calling and differential accessibility analysis of ATAC-seq were performed using the ATACofthesnake pipeline (https://github.com/maxplanck-ie/ATACofthesnake). Quality control and read mapping of RNA-seq were done using snakePipes (v2.5.1) (48). The expression level of the annotated genes (GRCm38.p4) was calculated by featureCounts (subread v2.0.0) (49). Intron counts were calculated as the difference between gene counts and exon counts for each gene. The differential gene expression was analyzed using the DESeq2 package (50), for exons and introns separately. Genes with a q-value < 0.05 were considered significantly differentially expressed.

Data, Materials, and Software Availability. The datasets generated during this study are available in the Gene Expression Omnibus (GEO) database under the accession number GSE201144: https://www.ncbi.nlm.nih.gov/geo/query/acc.cgi?acc=GSE201144.

ACKNOWLEDGMENTS. We thank the MPI Deep sequencing facility for sequencing and Dr. Ward Deboutte of the MPI Bioinformatics unit for help with the data analysis. We are grateful to Drs. C. Murre and Yina Zhou for advice on the dTAG system and Drs. Ritwick Sawarkar and Aurelie Lenaerts for discussions. The research was supported by funds of the Max Planck Society to R.G.

1. K. S. Zaret, Pioneer transcription factors initiating gene network changes. *Annu. Rev. Genet.* **54**, 367–385 (2020).
2. A. Mayran, J. Drouin, Pioneer transcription factors shape the epigenetic landscape. *J. Biol. Chem.* **293**, 13795–13804 (2018).
3. E. D. Larson, A. J. Marsh, M. M. Harrison, Pioneering the developmental frontier. *Mol. Cell* **81**, 1640–1650 (2021).
4. S. O. Dodonova, F. Zhu, C. Dienemann, J. Taipale, P. Cramer, Nucleosome-bound SOX2 and SOX11 structures elucidate pioneer factor function. *Nature* **580**, 669–672 (2020).
5. Z. Li *et al.*, Foxa2 and H2A.Z mediate nucleosome depletion during embryonic stem cell differentiation. *Cell* **151**, 1608–1616 (2012).
6. M. Iwafuchi *et al.*, Gene network transitions in embryos depend upon interactions between a pioneer transcription factor and core histones. *Nat. Genet.* **52**, 418–427 (2020).
7. C. Yan, H. Chen, L. Bai, Systematic study of nucleosome-displacing factors in budding yeast. *Mol. Cell* **71**, 294–305. e294 (2018).
8. J. Donaghey *et al.*, Genetic determinants and epigenetic effects of pioneer-factor occupancy. *Nat. Genet.* **50**, 250–258 (2018).
9. S. L. Nutt, B. L. Kee, The transcriptional regulation of B cell lineage commitment. *Immunity* **26**, 715–725 (2007).
10. S. Boller, R. Grosschedl, The regulatory network of B-cell differentiation: A focused view of early B-cell factor 1 function. *Immunol. Rev.* **261**, 102–115 (2014).
11. E. V. Rothenberg, Transcriptional control of early T and B cell developmental choices. *Annu. Rev. Immunol.* **32**, 283–321 (2014).
12. R. Li *et al.*, Dynamic EBF1 occupancy directs sequential epigenetic and transcriptional events in B-cell programming. *Genes Dev.* **32**, 96–111 (2018).
13. J. M. Pongubala *et al.*, Transcription factor EBF restricts alternative lineage options and promotes B cell fate commitment independently of Pax5. *Nat. Immunol.* **9**, 203–215 (2008).
14. D. Reynaud *et al.*, Regulation of B cell fate commitment and immunoglobulin heavy-chain gene rearrangements by Ikaros. *Nat. Immunol.* **9**, 927–936 (2008).
15. Y. C. Lin *et al.*, A global network of transcription factors, involving E2A, EBF1 and Foxo1, that orchestrates B cell fate. *Nat. Immunol.* **11**, 635–643 (2010).
16. C. Kadoch, G. R. Crabtree, Mammalian SWI/SNF chromatin remodeling complexes and cancer: Mechanistic insights gained from human genomics. *Sci. Adv.* **1**, e1500447 (2015).
17. C. Bossen *et al.*, The chromatin remodeler Brg1 activates enhancer repertoires to establish B cell identity and modulate cell growth. *Nat. Immunol.* **16**, 775–784 (2015).
18. Y. Wang *et al.*, A prion-like domain in transcription factor EBF1 promotes phase separation and enables B cell programming of progenitor chromatin. *Immunity* **53**, 1151–1167. e1156 (2020).
19. S. Boller *et al.*, Pioneering activity of the C-terminal domain of EBF1 shapes the chromatin landscape for B cell programming. *Immunity* **44**, 527–541 (2016).
20. S. Schick *et al.*, Acute BAF perturbation causes immediate changes in chromatin accessibility. *Nat. Genet.* **53**, 269–278 (2021).
21. M. Iurlaro *et al.*, Mammalian SWI/SNF continuously restores local accessibility to chromatin. *Nat. Genet.* **53**, 279–287 (2021).
22. K. Nishimura, T. Fukagawa, H. Takisawa, T. Kakimoto, M. Kanemaki, An auxin-based degron system for the rapid depletion of proteins in nonplant cells. *Nat. Methods* **6**, 917–922 (2009).
23. B. Nabet *et al.*, The dTAG system for immediate and target-specific protein degradation. *Nat. Chem. Biol.* **14**, 431–441 (2018).
24. A. Tallan, B. Z. Stanton, Inducible protein degradation to understand genome architecture. *Biochemistry* **60**, 2387–2396 (2021).
25. S. Roessler *et al.*, Distinct promoters mediate the regulation of Ebf1 gene expression by interleukin-7 and Pax5. *Mol. Cell. Biol.* **27**, 579–594 (2007).
26. T. Treiber *et al.*, Early B cell factor 1 regulates B cell gene networks by activation, repression, and transcription- independent poising of chromatin. *Immunity* **32**, 714–725 (2010).

27. C. R. Batista, S. K. Li, L. S. Xu, L. A. Solomon, R. P. DeKoter, PU.1 regulates Ig light chain transcription and rearrangement in pre-B cells during B cell development. *J. Immunol.* **198**, 1565–1574 (2017).
28. T. A. Schwickert *et al.*, Stage-specific control of early B cell development by the transcription factor Ikaros. *Nat. Immunol.* **15**, 283–293 (2014).
29. I. D. R. Revilla *et al.*, The B-cell identity factor Pax5 regulates distinct transcriptional programmes in early and late B lymphopoiesis. *EMBO J.* **31**, 3130–3146 (2012).
30. S. Yu *et al.*, BMP4 resets mouse epiblast stem cells to naive pluripotency through ZBTB7A/B-mediated chromatin remodelling. *Nat. Cell Biol.* **22**, 651–662 (2020).
31. J. Gilmour *et al.*, Robust hematopoietic specification requires the ubiquitous Sp1 and Sp3 transcription factors. *Epigenetics Chromatin* **12**, 33–43 (2019).
32. H. M. Layden, N. A. Eleuteri, S. W. Hiebert, K. R. Stengel, A protocol for rapid degradation of endogenous transcription factors in mammalian cells and identification of direct regulatory targets. *STAR Protoc.* **2**, 100530 (2021).
33. A. Ameur *et al.*, Total RNA sequencing reveals nascent transcription and widespread co-transcriptional splicing in the human brain. *Nat. Struct. Mol. Biol.* **18**, 1435–1440 (2011).
34. R. Nechanitzky *et al.*, Transcription factor EBF1 is essential for the maintenance of B cell identity and prevention of alternative fates in committed cells. *Nat. Immunol.* **14**, 867–875 (2013).
35. M. Iwafuchi-Doi, K. S. Zaret, Cell fate control by pioneer transcription factors. *Development* **143**, 1833–1837 (2016).
36. G. Hu *et al.*, Regulation of nucleosome landscape and transcription factor targeting at tissue-specific enhancers by BRG1. *Genome. Res.* **21**, 1650–1658 (2011).
37. H. W. King, R. J. Klose, The pioneer factor OCT4 requires the chromatin remodeller BRG1 to support gene regulatory element function in mouse embryonic stem cells. *Elife* **6**, e22631 (2017).
38. E. E. Swinstead, V. Paakinaho, D. M. Presman, G. L. Hager, Pioneer factors and ATP-dependent chromatin remodeling factors interact dynamically: A new perspective: Multiple transcription factors can effect chromatin pioneer functions through dynamic interactions with ATP-dependent chromatin remodeling factors. *Bioessays* **38**, 1150–1157 (2016).
39. M. O'Riordan, R. Grosschedl, Coordinate regulation of B cell differentiation by the transcription factors EBF and E2A. *Immunity* **11**, 21–31 (1999).
40. H. Maier *et al.*, Early B cell factor cooperates with Runx1 and mediates epigenetic changes associated with mb-1 transcription. *Nat Immunol* **5**, 1069–1077 (2004).
41. M. Sigvardsson *et al.*, Early B-cell factor, E2A, and Pax-5 cooperate to activate the early B cell-specific mb-1 promoter. *Mol. Cell. Biol.* **22**, 8539–8551 (2002).
42. N. R. Kong, M. Davis, L. Chai, A. Winoto, R. Tjian, MEF2C and EBF1 Co-regulate B cell-specific transcription. *PLoS Genet.* **12**, e1005845 (2016).
43. T. Maeda *et al.*, Regulation of B versus T lymphoid lineage fate decision by the proto-oncogene LRF. *Science* **316**, 860–866 (2007).
44. J. W. Steinke *et al.*, Identification of an Sp factor-dependent promoter in GCET, a gene expressed at high levels in germinal center B cells. *Mol. Immunol.* **41**, 1145–1153 (2004).
45. E. T. Friman *et al.*, Dynamic regulation of chromatin accessibility by pluripotency transcription factors across the cell cycle. *Elife* **8**, e50087 (2019).
46. S. L. McDaniel *et al.*, Continued activity of the pioneer factor zelda is required to drive zygotic genome activation. *Mol. Cell* **74**, 185–195. e184 (2019).
47. C. T. Jensen *et al.*, Dissection of progenitor compartments resolves developmental trajectories in B-lymphopoiesis. *J. Exp. Med.* **215**, 1947–1963 (2018).
48. V. Bhardwaj *et al.*, snakePipes: Facilitating flexible, scalable and integrative epigenomic analysis. *Bioinformatics* **35**, 4757–4759 (2019).
49. Y. Liao, G. K. Smyth, W. Shi, featureCounts: An efficient general purpose program for assigning sequence reads to genomic features. *Bioinformatics* **30**, 923–930 (2014).
50. M. I. Love, W. Huber, S. Anders, Moderated estimation of fold change and dispersion for RNA-seq data with DESeq2. *Genome. Biol.* **15**, 550 (2014).